Type of contribution:
Editorial
▶ Research Paper
Case Study
Review Paper
Scientific Data
Report of Tech. Application

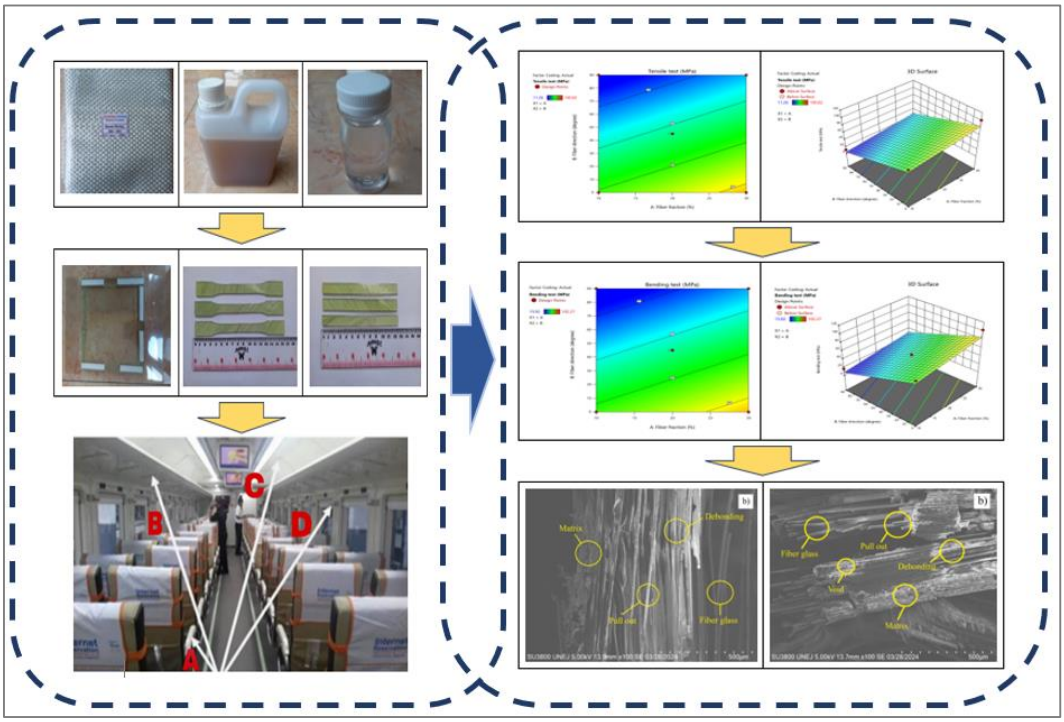
mesi
e-issn. 2798-5245

Mechanical Engineering for Society and Industry
Vol. 5, No. 2 (2025) pp 319-330
https://doi.org/10.31603/mesi.13090

Optimization of glass fiber reinforced polymer composite using response surface methodology for application on train panels

Yuni Hermawan[1]*, I Gusti Ketut Puja[2], Hendry Y. Nanlohy[3]

[1] Department of Mechanical Engineering, University of Jember, Jember 68121, **Indonesia**
[2] Department of Mechanical Engineering, Universitas Sanata Dharma, Sleman 55281, **Indonesia**
[3] Department of Mechanical Engineering, Jayapura University of Science and Technology, Jayapura 99351, **Indonesia**
✉ yunikaka@unej.ac.id



Highlights:

- The formation of composite from glass fiber reinforced polymer GFRP materials for train carriage composite panel applications.
- Tensile and bending test standards for train carriage composite panels are at least 75 kg/mm^2.
- The results of tensile and bending tests were 100.82 kg/mm^2 and 102.27 kg/mm^2. These test results meet composite standards for the use of panel materials for applications in train carriages.

Article info
Submitted: 2025-01-25
Revised: 2025-07-19
Accepted: 2025-12-28

This work is licensed under a Creative Commons Attribution-NonCommercial 4.0 International License

Publisher
Universitas Muhammadiyah Magelang

Abstract

Advancements in science and technology are creating challenges for conventional materials such as metals, often struggle to meet the demands of modern industry. In response to the issue, train industry has begun developing applications of Glass Fiber Reinforced Polymer (GFRP) composite for interior panels. Therefore, this research aimed to determine the impact of fiber volume fraction and arrangement direction on tensile as well as bending tests. This research also aimed to identify variations in composite manufacturing process parameters to achieve optimal tensile and bending strength values. The research methodology was an experimental procedure with data analysis using Statistics Software. During the analysis, the results showed that the fiber volume fraction of 30% with the fiber arrangement direction of 0° produced optimal tensile and bending strength values. Tensile and bending tests produced results of 100.82 kg/mm^2 and 102.27 kg/mm^2,

respectively. A high fiber volume fraction led to optimal tensile and bending strength values because the fiber served as the main reinforcement. Additionally, direction of the fiber arrangement played a significant role, with 0° fiber orientation producing better results due to a more even fiber distribution compared to 90° direction. The results of this research could be applied to the wall panels in the railway industry.

Keywords: Glass fiber reinforced polymer; Fiber volume fraction; Fiber arrangement direction; Tensile and bending strength; Composite manufacturing parameters

1. Introduction

Advancements in science and technology are creating challenges for conventional materials such as metals often struggle to meet the demands of modern industry. As a result, there has been a growing shift toward the use of composite materials, specifically in the industrial sector [1]. This rising trend is largely driven by the need for materials that offer specific and improved characteristics. Different from traditional metals, composite provide a unique combination of properties that are difficult to achieve, such as being lightweight, highly durable, resistant to corrosion, and easy to shape based on design requirements [2], [3], [4].

Composite is formed by combining two or more materials that have distinct mechanical properties. These materials work together, with one acting as the binder and the other as the reinforcement. The binder also known as the matrix can be made from metal, polymer, or ceramic, and it functions to hold composite together and distribute loads. Meanwhile, the reinforcing material plays a crucial role in supporting the structural load carried by composite. In polymer-based composite, reinforcement is typically provided in the form of fiber—among which fiberglass is one of the most commonly used [5], [6], [7].

The body of train carriage is made from light steel, which has several weaknesses. It is heavier than aluminum, prone to corrosion, and requires significant force to shape. To address these issues, the railway industry has begun adopting composite materials in train carriages. For instance, Glass Fiber Reinforced Polymer (GFRP) composite is used on the front end of train. Previous research also explores the use of GFRP composite for interior applications in train [8], [9], [10]. As a result, further research is needed to improve the mechanical properties of GFRP composite for train interiors [1], [11], [12]. The advantages of using GFRP composite for railway interior materials such as being lightweight, strong, and corrosion-resistant make the materials a suitable choice for modern train interiors. Moreover, there is growing interest in GFRP composite within the transportation industry, particularly for the potential to improve safety, durability, and aesthetic appeal.

The current research focuses on adjusting the fiber volume fraction and the orientation of fiber in GFRP composite to achieve optimal tensile and bending strength, verified through microstructural testing. For use in train interior panels, GFRP materials should meet specific standards, including a minimum tensile strength of 75 N/mm² and a minimum bending strength of 75 N/mm² [6]. An example of GFRP application in train design is shown in **Figure 1**.

The research questions in this result focus on how fiber volume fraction and arrangement direction affect the results of tensile as well as bending tests. Additionally, the research aims to identify the optimal process parameter variations for manufacturing composite with different fiber volume fraction as well as orientations to achieve the best possible tensile and bending strength. The main objective of this research is to optimize these parameters—fiber volume fraction and fiber direction—to obtain maximum tensile as well as bending performance.

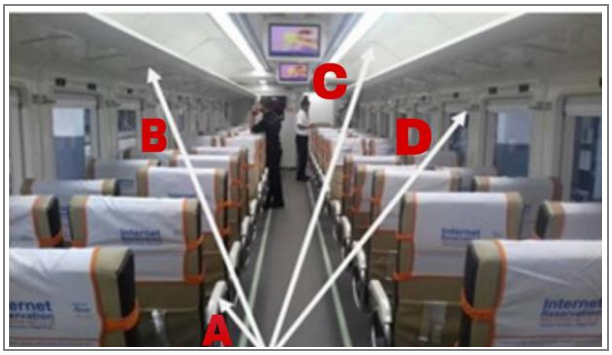


Figure 1. Application of GFRP on train: (a) Chair handrest; (b) Interior roof cover; (c) Side ceiling; (d) Courd cover

2. Methods

This research used an experimental method aimed at determining the optimal process parameter variations for achieving the best tensile and bending strength results. The parameters analyzed included fiber volume fraction and arrangement direction. To analyze these variations,

the research used Response Surface Methodology (RSM) with a Central Composite Design (CCD). Composite was fabricated using the hand lay-up method with glass mold. After composite specimens were formed, the samples were cut using a CNC Router machine following ASTM D638 standards. The tools and materials in this research consisted of the following.

- Research tools: Glass molds, Universal testing machine HT-2402 made in Taiwan, and Scanning electron microscope (SEM) Hitachi SU-3800 made in Japan.
- Research materials: Glass fiber, polyester Yucalac 157, and catalyst MEKPO.
- Composite manufacturing using the hand lay-up method
- Data processing using RSM method with CCD design.

The characteristics of the E-Glass material were shown in **Table 1** and the characteristics of polyester resin material were shown in **Table 2**. This research investigated three types of variables, namely independent, dependent, and controlled.

a. Independent variables were those whose measurements differed but were predetermined before the research was conducted. In this research, independent variables used were shown in **Table 3**.
b. Dependent variables consisted of variables whose values depended on the independent variables. The dependent variables in this research were tensile and bending test results.
c. Controlled variables were intentionally regulated or kept constant. The controlled variables in this research were composite manufacturing method using the hand lay-up method, the type of resin used was unsaturated polyester, and the fiber applied was woven roving.

Table 1. Characteristics of e-glass fiber

Properties	Value
Density	2.56 g/cm^3
Modulus of elasticity	72.5 GPa
Tensile strength	2712 MPa
Refractive index	1.55
Thermal conductivity	1 W/ m.K

Table 2. Characteristics of polyester resin

Properties	Value
Density	1.09 g/cm^3
Modulus elasticity	3.3 Gpa
Tensile strength	40 Mpa
Flexural strength	45 Mpa
Viscosity at 25 °C	250 cP

Table 3. Independent variables

Independent Variable	-1	0	+1
Fiber fraction	10%	20%	30%
Fiber direction	0°	45°	90°

The manufacturing process of glass fiber-reinforced polymer composite included the hand lay-up method. Specimens for tensile test were prepared according to ASTM D-638 standard [13], [14] and had the shape shown in **Figure 2**.

The dimensions of tensile test following ASTM D638, as shown in **Table 4**. The manufacturing of GFRP composite for bending tests followed ASTM D790 standard [15], [16], with the shape and dimensions as shown in **Figure 3**. The stages of SEM testing included sample preparation, observation using SEM, and analysis of the results. In addition, sample preparation included cutting the specimen to a size of 10 x 10 x 8 mm, cleaning it by blowing, and conducting observations at 100x magnification.

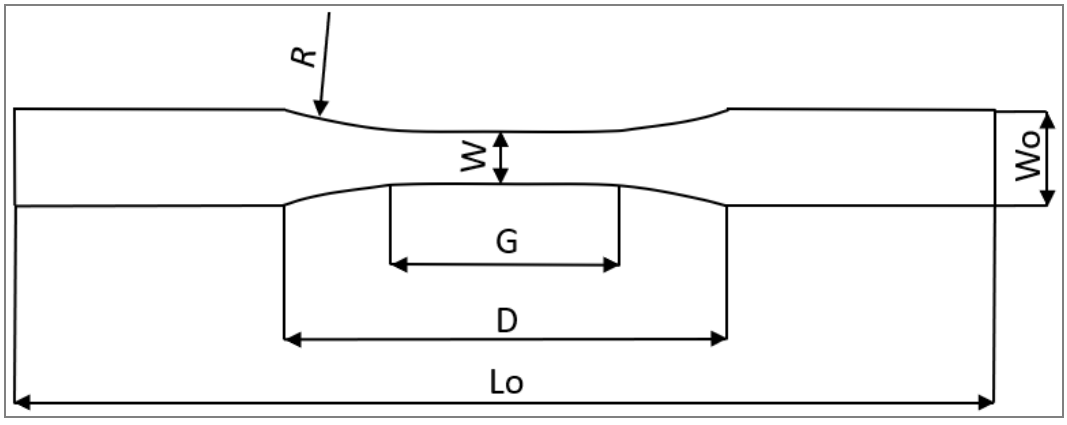


Figure 2. Tensile test specimen ASTM D638

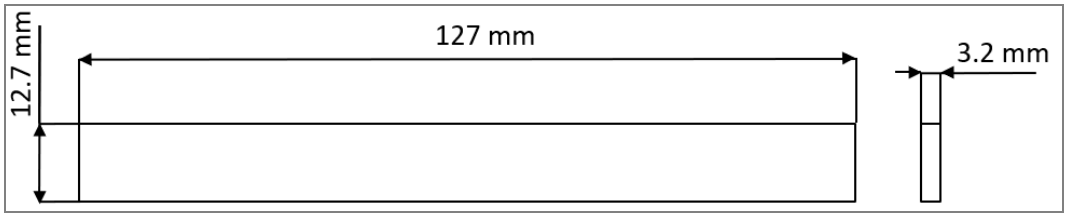


Figure 3. Bending test specimen ASTM D790

Table 4. Dimension specimen of tensile test

Dimensions	Length (mm)	Tolerance (mm)
W: *Width of narrow section*	13	±0.5
Wo: *Width of overall*	19	±0.5
Lo: *Length of overall*	165	No max
G: *Gage length*	50	±0.25
D: *Distance between grips*	115	±5
R: *Radius of fillet*	76	±1

3. Results and Discussion

3.1. Research Results

Composite specimens were prepared for tensile testing following ASTM D-638 standard, and for bending tests according to ASTM D-790, as shown in Figure 4. Composite specimens were initially produced as rectangular sheets using glass mold. The materials were then cut using a CNC Router machine, with the fiber arrangement direction carefully controlled according to the predetermined variations during the cutting process. Following the process, each test was replicated three times in this research. After performing tensile as well as bending tests, the results were compiled and shown in Table 5.

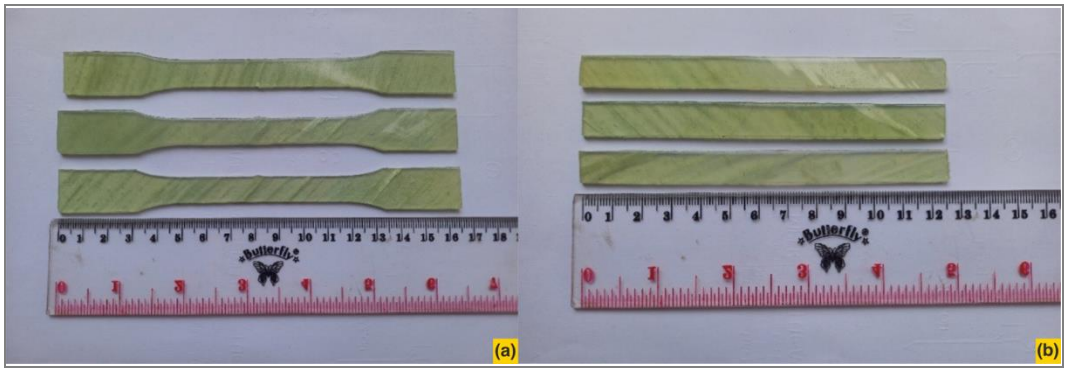


Figure 4. (a) Tensile test specimen ASTM D-638; (b) Bending test specimen ASTM D-790

Table 5. Tensile and bending test results

Standard	Run	Fiber fraction (%)	Fiber direction (°)	Tensile test (MPa)	Std Dev	Bending test (MPa)	Std Dev
9	1	20	45	34.44	1.17	38.00	1.22
13	2	20	45	33.03	0.53	33.14	1.96
12	3	20	45	41.75	1.12	39.89	0.29
7	4	20	-19	82.19	1.35	83.52	1.86
5	5	6	45	24.21	1.61	26.79	0.89
11	6	20	45	41.75	0.95	46.93	1.92
3	7	10	90	11.26	1.49	16.06	1.38
4	8	30	90	25.68	0.92	26.78	1.84
2	9	30	0	100.82	1.23	102.27	1.72
6	10	34	45	55.79	1.41	60.98	1.66
1	11	10	0	68.24	0.83	70.71	1.75
10	12	20	45	42.9	1.05	47.64	1.37
8	13	20	109	15.17	1.52	15.92	1.07

3.2. Discussion

3.2.1. Influence of Fiber Volume Fraction and Fiber Arrangement Direction on Tensile Test

Based on the data obtained, the highest tensile test result was achieved with the fiber volume fraction of 30% and the fiber arrangement direction of 0°, reaching a value of 100.82 MPa. This result showed that a higher fiber volume fraction led to greater tensile strength. Since fiber acted as reinforcements to bear applied loads, tensile strength was directly influenced by the amount of fiber volume fraction used.

The fiber arrangement direction also played a significant role in influencing tensile strength of the specimens. Specimens with fiber associated at 0° showed higher tensile and bending strength compared to those arranged at 90°. This difference occurred because the 0° fiber orientation allowed the load to be distributed more evenly along the fiber, while in the 90°

arrangement, the load tended to concentrate at the center. The fiber volume fraction affected tensile strength, with higher fiber content leading to increased tensile strength [17], [18].

Tensile test results were analyzed using RSM with CCD during the analysis. The statistical models available in Design Expert 13 software included linear, two-factor interaction (2FI), quadratic, and cubic models. Additionally, model selection was conducted to identify the most optimal response by evaluating the sequential model sum of squares, lack of fit, model summary statistics, and ANOVA results.

Data processed using Minitab software produced a normal distribution plot, shown in **Figure 5**. The results was concluded that the data followed a normal distribution since the p-value was greater than 0.05 with a p-value of 0.15.

Based on the sequential model sum of squares in **Table 6**, the Linear vs. Mean model was selected because it had the smallest p-value ($p < 0.0001$), which is less than 5%. This showed that the probability of a model error was less than 5%. Additionally, the selected model had a significant effect on tensile test response.

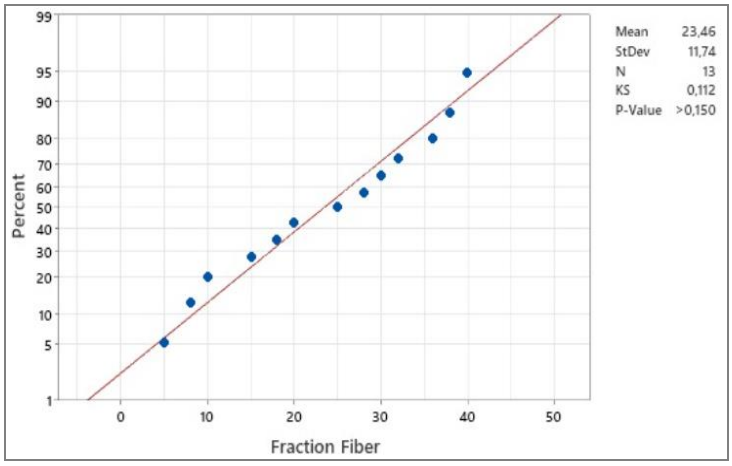


Figure 5. Normal distribution plot for fiber fraction

Table 7 showed the selected model based on the lack of fit. According to the table, the lack of fit for the Linear model was marked as "suggested," signifying that the model was selected. The F-value for the Linear model was smaller compared to those of the quadratic and cubic models. Although the 2FI model had a smaller F-value, the Linear model was selected because it had a higher sum of squares value.

Table 6. Sequential model sum of squares tensile test

Source	Sum of square	df	Mean square	F-value	p-value	
Mean vs linear	25630.34	1	25630.34			
Linear vs mean	7485.70	2	3742.85	48.04	<0.0001	Suggested
2FI vs linear	82.45	1	82.45	1.06	0.3290	
Quadratic vs 2FI	332.72	2	166.36	3.20	0.1031	
Cubic vs quadratic	174.96	2	87.48	2.31	0.1944	Aliased
Residual	189.05	5	37.81			
Total	33895.22	13	2607.32			

Table 7. Lack of fit tests tensile test

Source	Sum of square	df	Mean square	F-value	p-value	
Linear	692.67	6	115.44	5.34	0.0635	Suggested
2FI	610.22	5	122.04	5.64	0.0593	
Quadratic	277.49	3	92.50	4.28	0.0971	
Cubic	102.53	1	102.53	4.74	0.0950	Aliased
Pure error	86.51	4	21.63			

The model selection was based on the Model Summary Statistics, as shown in **Table 8**. The selected model was determined by evaluating several criteria. This included the smallest standard deviation, an R-squared value close to 1, highest adjusted R^2, highest predicted R^2, and lowest Prediction Error Sum of Squares (PRESS). According to the review, the program selected the Linear model, which had a standard deviation of 8.83—showing low variability in the data. Additionally, the PRESS value for the Linear model was lower than those of the 2FI, Quadratic, and Cubic models, which further supported its selection.

The results of the model selection analysis from all three methods consistently showed that the Linear model best represented the relationship between the fiber volume fraction and fiber arrangement direction variables as well as tensile test response. These methods included sequential model sum of squares, lack of fit tests, and model summary statistics.

The ANOVA analysis results in **Table 9** for tensile test response showed that the model was statistically significant, with a p-value less than 0.05. Specifically, the p-value for variable A (fiber volume fraction) was 0.0043, while variable B (fiber arrangement direction) had a p-value of less

than 0.0001. These results showed that both variables had a significant influence on tensile test response. The lack of fit test produced a p-value of 0.0635, which was greater than 5%.

Table 8. Model summary statistics tensile test

Source	Std. Dev	R^2	Adj R^2	Prd R^2	PRESS	
Linear	8.83	0.9057	0.8869	0.8225	1466.75	Suggested
2FI	8.80	0.9157	0.8876	0.7264	2261.39	
Quadratic	7.21	0.9560	0.9245	0.7449	2108.47	
Cubic	6.15	0.9771	0.9451	0.1897	6697.18	Aliased

Table 9. ANOVA for tensile test response

Source	Sum of squares	df	Mean square	F-value	p-value	
Model	7485.70	2	3742.85	48.04	<0.0001	Sig
A-Fiber fraction	1050.21	1	1050.21	13.48	0.0043	
B-Fiber orientation	6435.48	1	6435.48	82.59	<0.0001	
Residual	779.18	10	77.92	5.34		
Lack of fit	692.67	6	115.44		0.0635	Not sig
Pure error	86.51	4	21.63			
Cor total	8264.88	12				

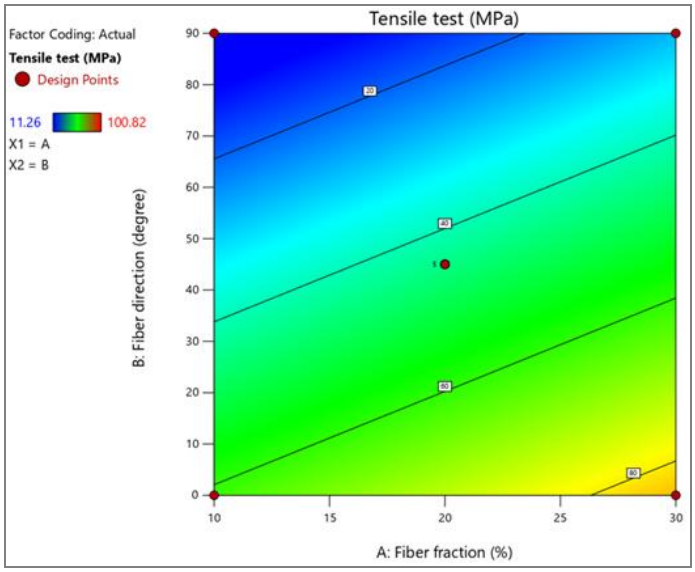


Figure 6. Contour plot of tensile test response

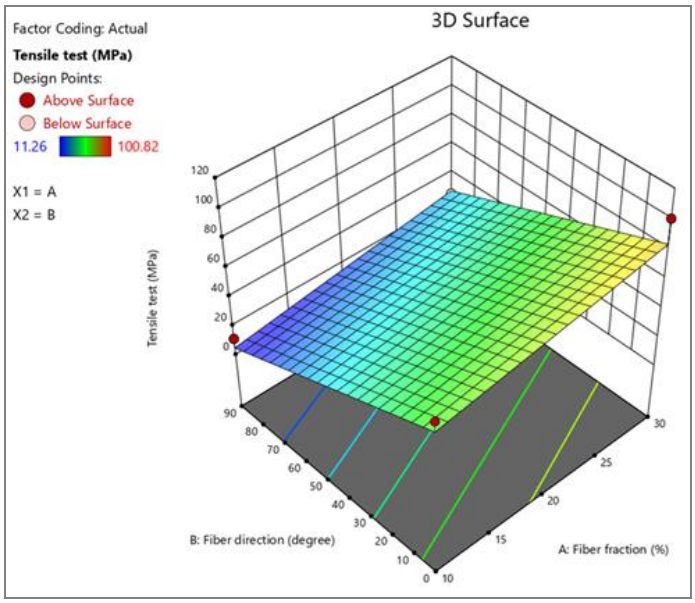


Figure 7. Surface plot of tensile test response

The response results were shown using contour lines in Figure 6. The most optimal tensile test values appeared in the red area located at the bottom right, corresponding to the fiber volume fraction of 30% and the fiber arrangement direction of 0°. As the fiber volume fraction decreased to 10% and the fiber arrangement direction shifted to 90º. This was represented by the blue area in the top left corner and tensile strength values progressively declined. The surface plot of the fiber volume fraction and fiber arrangement direction factors against tensile test response was shown in Figure 7.

The optimization results showed that the Linear model reached its peak performance at the fiber volume fraction of 30% and the fiber arrangement direction of 0°. As the fiber volume fraction decreased and the fiber orientation shifted further away from the position with direction of the applied load, tensile test response gradually declined. This trend confirmed that both a higher fiber volume and position with the load direction were critical for maximizing tensile strength.

3.2.2. Effect of Fiber Volume Fraction and Fiber Arrangement Direction on Bending Test

Based on the data obtained, the process was observed that an increase in fiber volume fraction led to a corresponding increase in bending strength. Specimens with fiber arranged along

the 0° direction supported the length of the specimen and showed higher bending strength. Meanwhile those with fibers oriented in the 90° direction showed a decrease in strength. The highest bending strength was recorded at 102.27 MPa in specimens with a 30% fiber volume fraction and a 0° fiber orientation. Consequently, the lowest bending strength, 15.92 MPa, was found in specimens with a 10% fiber volume fraction and a 90° fiber orientation. This trend occurred because the fiber served as both reinforcement and the main load-bearing component in composite. As a result, increasing the fiber volume fraction improved the ability of composite to resist bending loads [16], [19].

Bending test results were analyzed using RSM with CCD during this research. The statistical models available in Design Expert 13 software included Linear model, 2FI model, the Quadratic model, and Cubic model. To determine the optimal response, model selection was conducted based on several criteria, including the sequential model sum of squares, lack of fit tests, model summary statistics, and ANOVA results.

According to the sequential model sum of squares shown in **Table 10**, the Linear vs. Mean model was selected as the most appropriate. The decision was made because it had the smallest p-value, which was less than 0.0001 ($p < 5\%$). This showed that the probability of model error was less than 5%. The outcome confirmed that the selected model had a statistically significant influence on bending test response.

The selected model based on the lack of fit test was shown in **Table 11**. According to this table, the lack of fit results showed that the Linear model was the preferred choice. Additionally, the F-value for the Linear model was smaller compared to those of the 2FI, Quadratic, and Cubic models.

Model selection based on the Model Summary Statistics was shown in **Table 12**. The criteria for selecting the model included the smallest standard deviation, R-squared values closest to 1, the highest adjusted R^2 and predicted R^2, as well as the lowest Prediction Error Sum of Squares (PRESS). According to these statistics, the program selected the Linear model, which had a standard deviation of 9.02 and the lowest PRESS value compared to the 2FI, Quadratic, and Cubic models. This showed that the Linear model had low data variability and was the best fit among the options.

Table 10. Sequential model sum of squares bending test

Source	Sum of square	df	Mean square	F-value	p-value	
Mean vs linear	28494.65	1	28494.65			
Linear vs mean	7396.63	2	3698.32	45.45	<0.0001	Suggested
2FI vs linear	108.58	1	108.58	1.39	0.2693	
Quadratic vs 2FI	297.81	2	148.91	2.56	0.1465	
Cubic vs quadratic	153.73	2	76.86	1.52	0.3058	Aliased
Residual	253.51	5	50.70			
Total	36704.92	13	2823.46			

Table 11. Lack of fit tests bending test

Source	Sum of squares	df	Mean square	F-value	p-value	
Linear	662.44	6	110.41	2.92	0.1594	Suggested
2FI	553.86	5	110.77	2.93	0.1598	
Quadratic	256.04	3	85.35	2.26	0.2238	
Cubic	102.32	1	102.32	2.71	0.1753	Aliased
Pure error	151.19	4	37.80			

Table 12. Model summary statistics bending test

Source	Std. Dev	R^2	Adj R^2	Prd R^2	PRESS	
Linear	9.02	0.9009	0.8811	0.8207	1471.87	Suggested
2FI	8.85	0.9141	0.8855	0.7344	2180.57	
Quadratic	7.63	0.9504	0.9150	0.7495	2057.00	
Cubic	7.12	0.9691	0.9259	0.1737	6784.50	Aliased

The analysis of model selection using three methods consistently showed that the Linear model best represented the relationship between fiber volume fraction and fiber arrangement direction concerning bending test response. These methods included sequential model sum of squares, lack of fit tests, and model summary statistics.

The ANOVA results for bending test response shown in **Table 13** showed that the model was significant ($p < 0.05$). Variable A (fiber volume fraction) had a p-value of 0.0052, while variable B (fiber arrangement direction) had a p-value of less than 0.0001. These values showed that both fiber volume fraction and arrangement direction significantly influenced bending test response. The lack of fit test produced a p-value of 0.1594, which was greater than 5%.

Table 13. ANOVA for bending test response

Source	Sum of squares	Df	Mean square	F-value	p-value	
Model	7396.63	2	3698.32	45.45	<0.0001	Sig
A-Fiber fraction	1026.77	1	1026.77	12.62	0.0052	
B-Fiber orientation	6369.87	1	6369.87	78.29	<0.0001	
Residual	813.63	10	81.36	2.92		
Lack of fit	662.44	6	110.41		0.1594	Not sig
Pure error	151.19	4	37.80			
Cor total	8210.26	12				

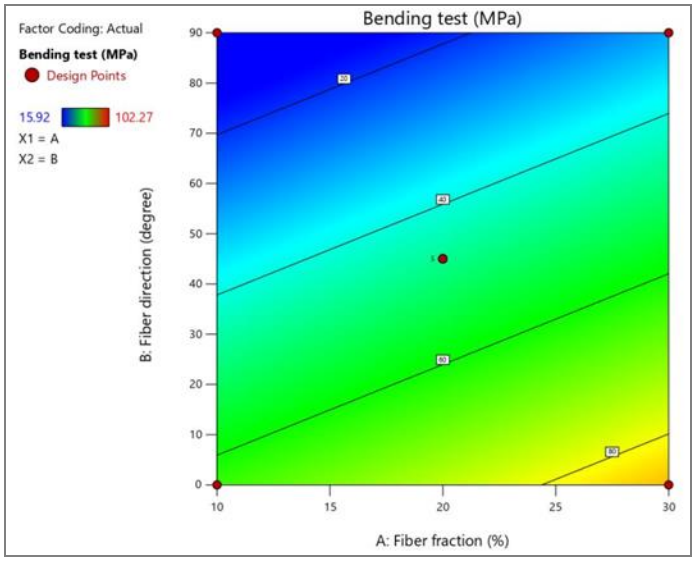


Figure 8. Contour plot of bending test response

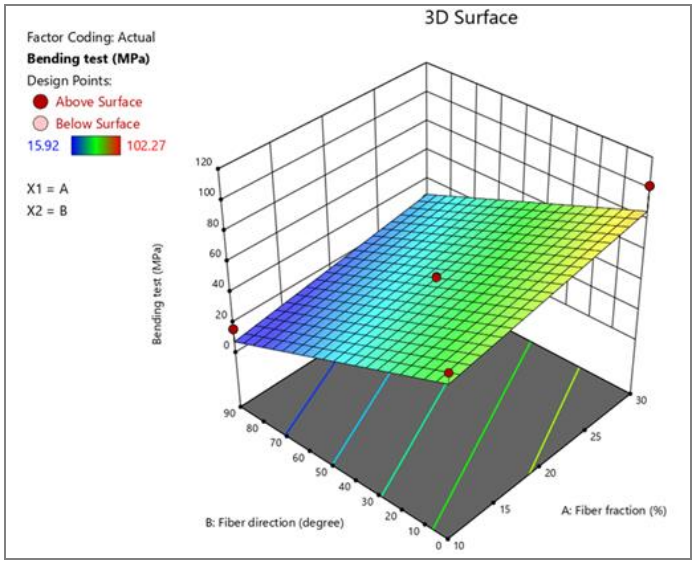


Figure 9. Surface plot of bending test response

Contour plot showing the influence of both factors, namely fiber volume fraction and fiber arrangement direction, on bending test response, as shown in **Figure 8**. The highest bending test result was observed along the contour line in the red-colored area at the bottom right corner. This corresponded to the fiber volume fraction of 30% and the fiber arrangement direction of 0°. The optimization results showed that the Linear model reached its peak performance under optimal conditions, specifically with the fiber volume fraction of 30% and the fiber arrangement direction of 0°. Outside this point, bending test response declined as the fiber volume fraction decreased and the fiber arrangement direction shifted further away from the position with the applied load on the specimen. This trend was shown by the surface curve showing the interaction between fiber volume fraction and arrangement direction on bending test response, as shown in **Figure 9**.

3.3. Optimizing Tensile and Bending Test Response

3.3.1. Optimization of Tensile Test Response

Optimization refers to a process conducted to obtain the most optimal results based on predetermined factors and response. Tensile test responded with a maximum target, as shown in **Table 14**. RSM provided optimization constraints to determine the optimal solution, as shown in **Table 15**.

The optimal tensile strength was achieved by using fiber volume fraction of 30% and the fiber arrangement direction of 0°, leading to a desirability value of 0.815.

Table 14. Optimization constraints

Criteria	Name (unit)	Target	Lower limit	Upper limit
Factor	Fiber fraction (%)	in range	10	30
Factor	Fiber direction (°)	in range	0	90
Respons	Tensile test (MPa)	Max	11.26	100.82

Table 15. Optimization solution

No	Fiber fraction (%)	Fiber direction	Tensile test	Desirability
1	30	0.000	84.222	0.815

3.3.2. Optimization of Bending Test Response

Optimization refers to the process conducted to obtain the most optimal results based on predetermined factors and response. Bending test responded with the maximum target, as shown in **Table 16**. Optimization constraints that were previously known could then determine the optimal solution using RSM, as shown in **Table 17**.

The results showed that the optimal bending strength was achieved with the fiber volume fraction of 30% and the fiber orientation of 0°, producing a desirability value of 0.816. Desirability represented the value of the optimization objective function, reflecting how well the program met the defined criteria. This value ranged from 0 to 1, with higher values showing a better position with the desired outcomes [20], [21].

Table 16. Optimization constraints

Criteria	Name (unit)	Target	Lower limit	Upper limit
Factor	Fiber fraction (%)	In range	10	30
Factor	Fibre direction (°)	In range	0	90
Respons	Bending test (MPa)	Max	15.92	102.27

Table 17. Optimization solution

No	Fiber fraction (%)	Fiber direction	Bending test	Desirability
1	30	0.000	86.364	0.816

3.4. Microscopic Test

Microscopic testing was performed to analyze the microstructure of the material using a SEM [22], [23], [24]. This examination aimed to observe the internal structure of GFRP composite that had passed through tensile and bending tests. Specifically, the test served to validate the results of these tests by correlating the examinations with the microstructural characteristics of specimens having varying fiber volume fraction and fiber orientations. **Figure 10** showed a section of tensile test specimen that was subjected to microscopic analysis. This analysis focused on identifying structural features and types of failure arising from the manufacturing process. It also provided an understanding of the quality of composite produced using the hand lay-up method. Moreover, the results in **Figure 10** showed the microstructural behavior of the specimens after tensile testing.

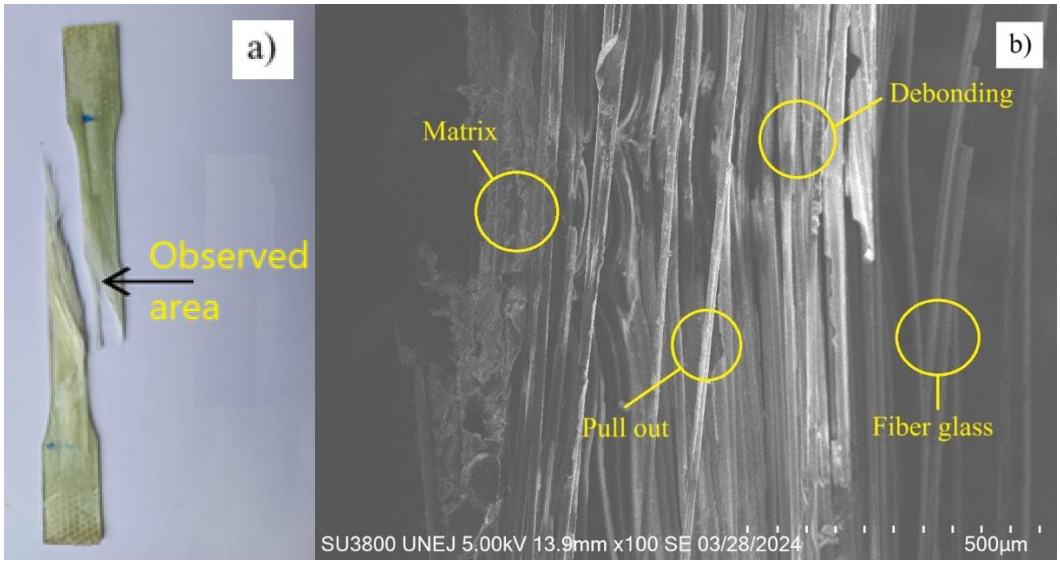


Figure 10. Tensile test result: (a) Fracture area; (b) SEM observation of the fracture site

The material used for bending test passed through microscopic examination near the fracture area of the specimen, as shown in **Figure 11**. The results of bending test were further analyzed under a microscope to assess the properties of the material and identify the types of failure caused by the hand lay-up process.

Based on the microscopic test results of tensile and bending specimens, several types of defects were observed, including voids, fiber pull-outs, and debonding. Voids appeared as air pockets in composite material, caused by trapped air during the manufacturing process. These voids compromised the integrity of composite by forming cavities in the final product. Fiber pull-

out occurred as the bond between the fiber and the matrix weakened under increasing loads. This showed that the fiber had become more ductile, allowing the load to transfer and eventually causing the materials to be pulled out [5], [25]. Another type of failure observed was debonding caused by weak adhesion between the matrix and the fiber, which reduced the total quality of composite. The dominant failure mode appeared to be fiber pull-out, as shown by visible fiber fractures and inconsistent fiber sizes. This failure was evident in the SEM images, which showed the fiber detaching from the matrix. Interfacial debonding was identified as the primary fracture type, with glass fiber visibly separated from the matrix in the examined specimens [5], [26], [27].

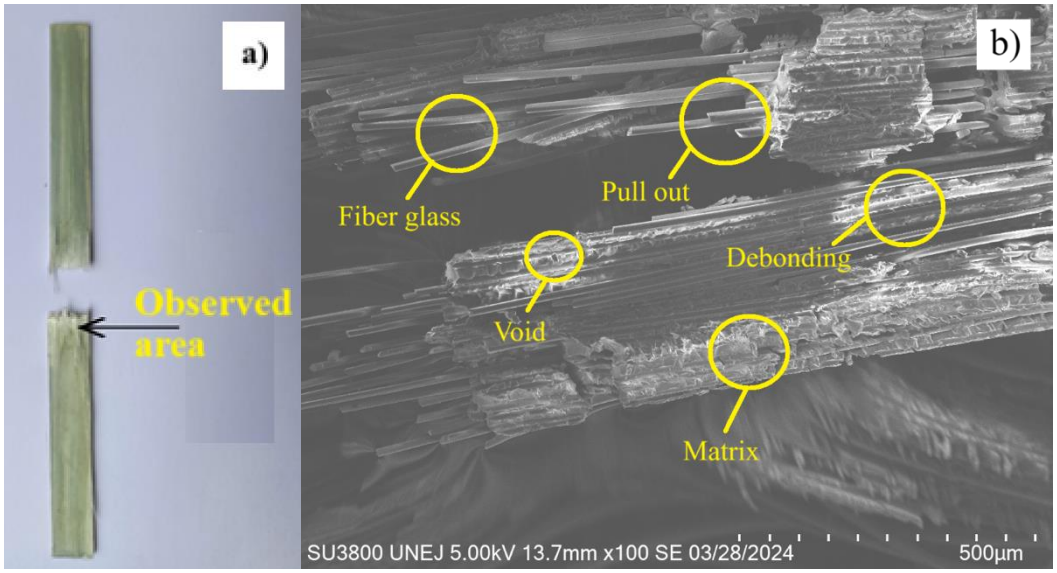


Figure 11. Bending test result: (a) Fracture area; (b) SEM observation of the fracture site

4. Conclusion

In conclusion, several assumptions were drawn based on the results of the conducted research which included the following.

a. The optimal parameters to achieve the maximum tensile strength included the fiber volume fraction of 30% with the fiber orientation of 0°, leading to a desirability value of 0.815.
b. Tensile strength and bending strength of GFRP composite were 100.82 N/mm² and 102.27 N/mm², respectively. Both values exceeded the standard requirements for railway interior panels.
c. SEM observations showed that glass fiber were pulled out, debonded, and void in composite matrix, leading to less than maximum tensile as well as bending strength. The failure due to fibers being pulled out of the matrix, matrix and fibers being peeled off. This failure was due to the weak bond between the fibers and the matrix due to the tensile force load.

5. Suggestions for Further Research

Further research would be specifically needed to develop more innovative fabrication methods for GFRP fiber composite. These advancements would improve the potential of the material to meet the demands of the railway industry by making manufacturing easier and more efficient. Additionally, applying vacuum methods could help reduce defects during production.

Acknowledgements

The authors are grateful to LP2M University of Jember - Indonesia for providing an Internal Research Grant that supported the successful completion of this work.

Authors' Declaration

Authors' contributions and responsibilities - The authors made substantial contributions to the conception and design of the study. The authors took responsibility for data analysis, interpretation and discussion of results. The authors read and approved the final manuscript.

Funding – LP2M University of Jember - Indonesia.

Availability of data and materials - All data is available from the authors.

Competing interests - The authors declare no competing interests.

Additional information – No additional information from the authors.

References

[1] M. R. Gunarti, A. Prawoto, W. N. Fauzi, and W. A. Wirawan, "Mechanical behavior of glass fiber-epoxy composite laminates for ship hull structures," *Mechanical Engineering for Society and Industry*, vol. 4, no. 2, pp. 156–166, Nov. 2024, doi: 10.31603/mesi.11589.

[2] S. Kumarasamy, M. S. Zainol Abidin, M. N. Abu Bakar, M. S. Nazida, Z. Mustafa, and A. Anjang, "Effects of High and Low Temperature on the Tensile Strength of Glass Fiber Reinforced Polymer Composites," *IOP Conference Series: Materials Science and Engineering*, vol. 370, p. 012021, May 2018, doi: 10.1088/1757-899X/370/1/012021.

[3] A. Önder and M. Robinson, "Investigating the feasibility of a new testing method for GFRP/polymer foam sandwich composites used in railway passenger vehicles," *Composite Structures*, vol. 233, p. 111576, Feb. 2020, doi: 10.1016/j.compstruct.2019.111576.

[4] Y. Pan and D. Yan, "Study on the durability of GFRP bars and carbon/glass hybrid fiber reinforced polymer (HFRP) bars aged in alkaline solution," *Composite Structures*, vol. 261, p. 113285, Apr. 2021, doi: 10.1016/j.compstruct.2020.113285.

[5] M. Y. Zaghloul, M. M. Y. Zaghloul, and M. M. Y. Zaghloul, "Influence of Stress Level and Fibre Volume Fraction on Fatigue Performance of Glass Fibre-Reinforced Polyester Composites," *Polymers*, vol. 14, no. 13, p. 2662, Jun. 2022, doi: 10.3390/polym14132662.

[6] M. Nikam *et al.*, "Optimization of Machining Parameters for Enhanced Performance of Glass-Fibre-Reinforced Plastic (GFRP) Composites Using Design of Experiments," *Sustainability*, vol. 15, no. 16, p. 12372, Aug. 2023, doi: 10.3390/su151612372.

[7] H. Gao, Y. Sun, J. Jian, Y. Dong, and H. Liu, "Study on mechanical properties and application in communication pole line engineering of glass fiber reinforced polyurethane composites (GFRP)," *Case Studies in Construction Materials*, vol. 18, p. e01942, Jul. 2023, doi: 10.1016/j.cscm.2023.e01942.

[8] W. D. Callister and D. G. Rethwisch, *Materials science and engineering: an introduction*, vol. 9. Wiley New York, 2018.

[9] P. Morampudi, K. K. Namala, Y. K. Gajjela, M. Barath, and G. Prudhvi, "Review on glass fiber reinforced polymer composites," *Materials Today: Proceedings*, vol. 43, pp. 314–319, 2021, doi: 10.1016/j.matpr.2020.11.669.

[10] O. Tengilimoglu and U. Akyuz, "Experimental study on hybrid precast tunnel segments reinforced by macro-synthetic fibres and glass fibre reinforced polymer bars," *Tunnelling and Underground Space Technology*, vol. 106, p. 103612, Dec. 2020, doi: 10.1016/j.tust.2020.103612.

[11] A. Saeedi, M. Motavalli, and M. Shahverdi, "Recent advancements in the applications of fiber-reinforced polymer structures in railway industry—A review," *Polymer Composites*, vol. 45, no. 1, pp. 77–97, Jan. 2024, doi: 10.1002/pc.27817.

[12] C. Yang, Y. Gao, W. Guo, Y. Yang, P. Xu, and M. S. Alqahtani, "High-velocity impact behaviour of curved GFRP composites for rail vehicles: Experimental and numerical study," *Polymer Testing*, vol. 116, p. 107774, Dec. 2022, doi: 10.1016/j.polymertesting.2022.107774.

[13] ASTM Standart D638-14, "Standard Test Method for Tensile Properties of Plastics," Dec. 15, 2014, *ASTM International, West Conshohocken, PA*. doi: 10.1520/D0638-14.

[14] G.-V. Săftoiu, C. Constantin, A.-I. Nicoară, G. Pelin, D. Ficai, and A. Ficai, "Glass Fibre-Reinforced Composite Materials Used in the Aeronautical Transport Sector: A Critical Circular Economy Point of View," *Sustainability*, vol. 16, no. 11, p. 4632, May 2024, doi: 10.3390/su16114632.

[15] ASTM Standart D790, "Standard Test Methods for Flexural Properties of Unreinforced and Reinforced Plastics and Electrical Insulating Materials," Apr. 01, 2010, *ASTM International, West Conshohocken, PA*. doi: 10.1520/D0790-10.

[16] A. Özdemir and A. Önder, "An environmental life cycle comparison of various sandwich composite panels for railway passenger vehicle applications," *Environmental Science and Pollution Research*, vol. 27, no. 36, pp. 45076–45094, Dec. 2020, doi: 10.1007/s11356-020-10352-8.

[17] A. Parmiggiani, M. Prato, and M. Pizzorni, "Effect of the fiber orientation on the tensile and flexural behavior of continuous carbon fiber composites made via fused filament fabrication," *The International Journal of Advanced Manufacturing Technology*, vol. 114, no. 7–8, pp. 2085–2101, Jun. 2021, doi: 10.1007/s00170-021-06997-5.

[18] A. Equbal *et al.*, "Application of the Combined ANN and GA for Multi-Response Optimization of Cutting Parameters for the Turning of Glass Fiber-Reinforced Polymer Composites," *Mathematics*, vol. 8, no. 6, p. 947, Jun. 2020, doi: 10.3390/math8060947.

[19] G. Rathnakar and H. K. Shivanand, "Fibre Orientation and Its Influence on the Flexural Strength of Glass Fibre and Graphite Fibre Reinforced Polymer Composites," *International Journal of Innovative Research in Science,Engineering and Technology*, vol. 2, no. 3, pp. 548–552, 2013.

[20] M. Mobin, S. M. Mousavi, M. Komaki, and M. Tavana, "A hybrid desirability function approach for tuning parameters in evolutionary optimization algorithms," *Measurement*, vol. 114, pp. 417–427, Jan. 2018, doi: 10.1016/j.measurement.2017.10.009.

[21] S. Dasari, S. Lohani, S. Sumit Dash, A. Omprakash Fulmali, R. Kumar Prusty, and B. Chandra Ray, "A novel study of flexural behavior of short glass fibers as secondary reinforcements in GFRP composite," *Materials Today: Proceedings*, vol. 47, pp. 3370–3374, 2021, doi: 10.1016/j.matpr.2021.07.161.

[22] Y. Hermawan, R. Soenoko, Y. Irawan, and S. Setyabudi, "Minimizing Temperature And Tool Wear On Rock Cutting With Negative Rake Angle," *MM Science Journal*, vol. 2019, no. 2, pp. 2927–2934, Jun. 2019, doi: 10.17973/MMSJ.2019_06_2019004.

[23] Y. Hermawan, R. Soenoko, Y. S. Irawan, and S. A. Setyabudi, "Cutting Forces, Chips Formation and Surface Roughness in Rock Cutting Using Negative Rake Angle," *Manufacturing Technology*, vol. 20, no. 1, pp. 27–35, Aug. 2020, doi: 10.21062/mft.2020.009.

[24] D. K. Rajak, P. H. Wagh, and E. Linul, "Manufacturing Technologies of Carbon/Glass Fiber-Reinforced Polymer Composites and Their Properties: A Review," *Polymers*, vol. 13, no. 21, p. 3721, Oct. 2021, doi: 10.3390/polym13213721.

[25] W. Ferdous *et al.*, "Static behaviour of glass fibre reinforced novel composite sleepers for mainline railway track," *Engineering Structures*, vol. 229, p. 111627, Feb. 2021, doi: 10.1016/j.engstruct.2020.111627.

[26] M. A. Verstraete, W. De Waele, R. M. Denys, K. Van Minnebruggen, and S. Hertelé, "Constraint analysis of defects in strength mismatched girth welds of (pressurized) pipe and Curved Wide Plate tensile test specimens," *Engineering Fracture Mechanics*, vol. 131, pp. 128–141, Nov. 2014, doi: 10.1016/j.engfracmech.2014.07.018.

[27] F. Xie, W. Tian, S. Li, P. Diez, S. Zlotnik, and A. G. Gonzalez, "Experimental Study on the Structural Performance of Glass-Fiber-Reinforced Concrete Slabs Reinforced with Glass-Fiber-Reinforced Polymer (GFRP) Bars: A Sustainable Alternative to Steel in Challenging Environments," *Polymers*, vol. 17, no. 8, p. 1068, Apr. 2025, doi: 10.3390/polym17081068.